Numerical Investigation of Unsaturated Frozen Soil Behavior Under Cyclic Freeze-Thaw Conditions

Emad Norouzi*,1 and Biao Li1

1*Department of Building, Civil & Environmental Engineering, Concordia University, Montreal, Quebec, Canada*

**Corresponding author's email:* emad.norouzi@concordia.ca

Abstract: This study presents a numerical model to investigate the behavior of unsaturated frozen soil under cyclic freeze-thaw conditions, with validation against experimental data. Governing equations for mass, momentum, and energy conservation were coupled with a Soil Freezing Characteristic Curve (SFCC) model to account for temperature and capillary pressure dependencies. The numerical simulation focused on a 2D plane strain problem using the Finite Element Method and a fully implicit time integration scheme. Results revealed consistent temperature distribution patterns. The displacement analysis showed frost heave during freezing and settlement during thawing, with a wider range of variations during the second cycle. Differences between the two cycles were attributed to residual plastic deformation water pressure redistribution in the medium. The proposed model provides valuable insights for understanding and mitigating the effects of freeze-thaw cycles in geotechnical engineering, offering a reliable framework for analyzing soil behavior in cold regions.

Introduction

Frozen soil, generally composed of soil, ice, and water, is classified into two types: saturated soils, which lack air, and unsaturated soils, which contain air within their structure. In both categories, freezing can result in frost heave, leading to an expansion in soil volume. This occurs as freezing enhances water migration and crystallization, causing soil particles to separate. Understanding the deformation of frozen soil and permafrost is crucial, as it directly impacts the stability of infrastructure, such as buildings, roads, and pipelines, in cold regions. Moreover, with climate change accelerating permafrost thaw, these deformations pose increasing risks to both engineered systems and natural ecosystems.

Unlike in saturated soils, frost heave prediction for unsaturated soils must also account for factors like air flux [1]. Numerical modeling of unsaturated frozen soil during freeze-thaw cycles is vital for predicting and mitigating these impacts, providing insights into soil behavior under varying environmental and engineering conditions. Current THM models for frozen soils predominantly address fully saturated geomaterials, focusing on freezing and thawing processes, frost heave, and cryo-suction effects [2,3]. Recently, there has been an increasing

focus on coupled THM models for unsaturated soils. Bai et al. (2020) proposed a frost heave model that incorporates an effective strain ratio to relate frost heave strain to moisture and temperature fields [4]. Huang and Rudolph (2021) introduced a model for variably saturated soils, linking ice lens segregation, stress-deformation, and void ratio evolution [5]. Their model, validated with experimental data, included vapor transport but simplified dry air movement. Wu and Ishikawa (2022) developed a THM model for partially saturated frost-susceptible soils, demonstrating that frost heave is influenced by saturation, cooling rates, and overburden pressure [6]. Applying pore water, ice, and air pressures to fully define effective stress laws, and incorporating phase change strain, Li et al. (2024) verified their numerical model with field data using a poro-elastic THM model [7]. Norouzi and Li (2024) introduced a coefficient to adjust the phase change strain in an unsaturated frozen medium and developed a poro-plastic numerical model, which they validated with experimental data [8]. This study investigates the effect of cyclic freeze-thaw actions on the displacement of unsaturated frozen soil using a poro-plastic numerical THM model.

Volumetric relations

The volumetric content of each phase (soil, water, ice, and moist air), denoted as θ_α, is calculated as the ratio of the phase's volume (V_α) to the total volume (V):

$$\theta_\alpha = \frac{V_\alpha}{V} \tag{1}$$

Porosity, n, is the ratio of void volume to total volume, while the saturation of each phase (S_α) is defined as the ratio of its volumetric content to the porosity, with the sum of all saturations equal to unity.

Governing Equations

In this section the governing equations for unsaturated frozen soil have been introduced. The details of the equations can be found in [8].

Linear momentum equation

Equation 2 describes the conservation of linear momentum in porous media, ensuring the balance between the divergence of the total stress tensor ($\boldsymbol{\sigma}$) and body force ($\mathbf{b}$):

$$\nabla \cdot \boldsymbol{\sigma} + \mathbf{b} = \mathbf{0} \tag{2}$$

According to Yin et al. (2023), the total stress can be approximated as a combination of effective stress ($\boldsymbol{\sigma}'$) and pore pressure components, weighted by their respective saturations [9]:

$$\boldsymbol{\sigma} = \boldsymbol{\sigma}' - S_w P_w \mathbf{I} - S_g P_g \mathbf{I} - S_i P_i \mathbf{I} \tag{3}$$

Here, the saturations of water (S_w), air (S_g), and ice (S_i) serve as weight coefficients for their corresponding pore pressure components (P_w, P_g, and P_i).

Mass balance equation of water species

The conservation of mass for water, ice, and vapor can be combined under the assumption that the mass changes of water and ice are equal but opposite during freezing and thawing. By incorporating Darcy's law, the governing equation is expressed as [10]:

$$\begin{aligned} S_g \frac{\partial \rho_{gw}}{\partial t} + n\rho_{gw} \frac{\partial S_g}{\partial t} + n\rho_w \frac{\partial S_w}{\partial t} + n\rho_i \frac{\partial S_i}{\partial t} - \nabla \cdot \left(\rho_g \frac{M_a M_w}{{M_g}^2} \mathbf{D}_{gw} \nabla \left(\frac{P_{gw}}{P_g} \right) \right) - \nabla \\ \cdot \left(\rho_w \frac{\mathbf{k} k_{rw}}{\mu_w} (\nabla P_w - \rho_w \mathbf{g}) \right) - \nabla \cdot \left(\rho_{gw} \frac{\mathbf{k} k_{rg}}{\mu_g} (\nabla P_g - \rho_g \mathbf{g}) \right) - \beta_{swgi} \frac{\partial T}{\partial t} \\ + (S_w \rho_w + S_g \rho_{gw} + S_i \rho_i) \nabla \cdot \mathbf{v}_s = 0 \end{aligned} \tag{4}$$

This equation integrates mass conservation while accounting for phase change dynamics, fluid flow governed by Darcy's law, and the effects of thermal gradients and deformation.

Mass balance equation of dry air

The mass balance equation for dry air is [10]:

$$\begin{aligned} n S_g \frac{\partial \rho_{ga}}{\partial t} + n\rho_{ga} \frac{\partial S_g}{\partial t} + S_g \rho_{ga} \nabla \cdot \mathbf{v}_s + \nabla \cdot \left(\rho_g \frac{M_a M_w}{{M_g}^2} \mathbf{D}_{gw} \nabla \left(\frac{P_{gw}}{P_g} \right) \right) - \nabla \\ \cdot \left(\rho_{ga} \frac{\mathbf{k} k_{rg}}{\mu_g} (\nabla P_g - \rho_g \mathbf{g}) \right) - \beta_{sg} \frac{\partial T}{\partial t} = 0 \end{aligned} \tag{5}$$

Here, the solid particle velocity is given by $\mathbf{v}_s = d\mathbf{u}/dt$, where $\mathbf{u}$ represents the medium's displacement. The coefficients β_{swgi} and β_{sg} denote the equivalent thermal expansion factors for mass changes in the unsaturated frozen soil and solid-air mixture, respectively.

Energy balance equation

The energy balance equation for the medium, assuming local thermodynamic equilibrium for all components, is expressed as [1]:

$$\left(\rho C_p\right)_{\text{eff}} \frac{\partial T}{\partial t} + \mathbf{a} \cdot \nabla T - \nabla \cdot (\lambda_{\text{eff}} \nabla T) - L_f \rho_i \frac{\partial \theta_i}{\partial t} = 0 \tag{6}$$

Here, L_f is the latent heat coefficients for the water-ice phase change. The terms $\left(\rho C_p\right)_{\text{eff}}$ and λ_{eff} represent the effective heat capacity and thermal conductivity, respectively. Additionally, $\mathbf{a}$ represents the advection vector for heat transfer, dependent on the relative velocities of water-solid ($\mathbf{v}_{w,s}$) and air-solid ($\mathbf{v}_{g,s}$):

$$\mathbf{a} = nS_w\rho_w C_p^w \mathbf{v}_{w,s} + nS_g\rho_g C_p^g \mathbf{v}_{g,s} \tag{7}$$

Constitutive relations

Modified Clausius-Clapeyron equation

The modified Clausius-Clapeyron equation is based on thermodynamic equilibrium and describes the relationship between temperature, ice pressure, and pore water pressure in partially frozen soil [8].

$$\frac{L_f}{T_0} dT = \frac{dP_{wf}}{\rho_w} - \frac{dP_i}{\rho_i} \tag{8}$$

In Equation (8), ρw and ρi are the densities of water and ice, respectively and $T_0 = 273$ K represents the reference temperature. Equation (8) is derived from the equilibrium condition between ice and water phases, modified to account for suction effects in unsaturated conditions. This thermodynamic basis is consistent with the assumptions of the SFCC model, which describes saturation changes under coupled temperature and capillary pressure.

Soil freezing characteristics curve

To calculate water, ice, and air saturations in an unsaturated frozen medium, a Soil Freezing Characteristic Curve (SFCC) model is developed based on Soil Water Characteristic Curve (SWCC) models. The Van Genuchten (1980) model is employed to estimate water, ice, and air saturations as functions of capillary pressure and temperature [11]. This model accurately accounts for the interplay between capillary pressure (P_c) and temperature, enhancing the reliability of predictions in unsaturated frozen media.

- Above freezing point temperature:

$$\theta_w = \theta_r + (\theta_s - \theta_r)(1 + [\alpha_v P_c]^{n_v})^{-m_v}$$
$$S_w = \frac{\theta_w}{n}, \qquad S_g = 1 - S_w \tag{9}$$

- Under freezing point temperature:

$$\theta_{tw} = \theta_r + (\theta_s - \theta_r)\left(1 + \left[\alpha_v \frac{P_c}{\beta}\right]^{n_v}\right)^{-m_v}$$
$$\theta_w = \theta_r + (\theta_s - \theta_r)\left(1 + \left[\alpha_v \left(\frac{P_c}{\beta} + \rho_w \frac{L_f}{T_0}(T_f - T)\right)\right]^{n_v}\right)^{-m_v} \tag{10}$$

$$\theta_i = \frac{\rho_w}{\rho_i}(\theta_{tw} - \theta_w)$$

$$S_w = \frac{\theta_w}{n}, \qquad S_i = \frac{\theta_i}{n}, \qquad S_g = 1 - S_w - S_i$$

In above equations, n_v, m_v, and α_v are model parameters which can be found by fitting the curves of SWCC.

Phase change strain

The following relationship can be used to relate effective stress and effective strain:

$$\mathrm{d}\boldsymbol{\sigma}' = \mathbf{D}_{\mathrm{T}}\left(d\boldsymbol{\varepsilon} - d\boldsymbol{\varepsilon}^{\mathrm{ph}} - d\boldsymbol{\varepsilon}^{T}\right) \tag{11}$$

where $\mathbf{D}_{\mathrm{T}}$ is the tangential constitutive matrix, dϵ is the total strain increment vector, and $d\boldsymbol{\varepsilon}^{T}$ is thermal strain increment. Additionally, considering β_{ph} ($0 < \beta_{\mathrm{ph}} < 1$) as an adjustment coefficient [8], strain increment due to phase change ($d\boldsymbol{\varepsilon}^{\mathrm{ph}}$) for unsaturated freezing conditions is modified as:

$$d\boldsymbol{\varepsilon}^{\mathrm{ph}} \cong \frac{\beta_{\mathrm{ph}}}{3}\left(\frac{n(\rho_w - \rho_i)}{\rho_w S_w + \rho_i S_i} dS_i\right)\mathbf{I} \tag{12}$$

β_{ph} was calibrated empirically as suggested in [8]. It accounts for volumetric discrepancies for phase change in an unsaturated medium since in an unsaturated medium, a portion of volumetric expansion due to freezing allocates to fill into the unsaturated pores [4].

In this simulation the Drucker-Prager model is implemented with an associative flow rule to capture plastic strains due to stress exceeding yield surfaces. Details can be found in [8].

Numerical simulation

After presenting the governing and auxiliary equations, the weak forms of these equations need to be derived. Considering both essential and natural boundary conditions, the coupled equations are discretized into a nonlinear differential equation over time. $\mathbf{u}$, P_w, P_g, T are the primary variables, with coefficients dependent on these parameters, resulting in highly nonlinear equations. A fully implicit time discretization method is employed, solved using a Newton-Raphson scheme within the Finite Element Method (FEM). The current numerical model has been validated against various test cases [7,8]. Also, a mesh convergence analysis confirmed that a finer mesh yielded negligible differences [12]. In this study, a new simulation has been developed to analyze the effects of cyclic freeze-thaw actions.

Sample setup and material properties

In order to investigate the deformation of unsaturated frozen soil under cyclic freezing and thawing, a 2D plane strain model was constructed based on the derived equations. The sample

dimensions and material properties used in the simulation were taken from an experiment conducted by [4]. As shown in Figure 1, the sample measures 5 cm × 9 cm, with a mesh size of 0.5 cm × 0.5 cm.

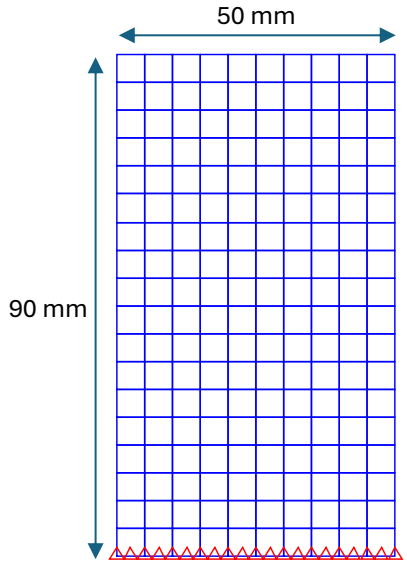

Figure 1: Numerical meshing and boundary conditions of the simulation

The sample's initial total water content is 0.23, and the pore water pressure is distributed hydrostatically. The thermal and hydraulic properties of the model, obtained from references, are provided in Table 1 [4]. For the mechanical behavior, an associative Drucker-Prager model with temperature-dependent soil properties was adopted [4,13].

Table 1: Material properties of the simulation

Initial porosity	$n = 0.47$ (-)
Density of solid	$\rho_s = 2700$ (kg/m^3)
Density of ice	$\rho_i = 910$ (kg/m^3)
Density of water	$\rho_w = 1000$ (kg/m^3)
Intrinsic permeability	$\mathbf{k} = 8 \times 10^{-13}$ (m^2)
Van Genuchten's model parameter	$\alpha_v = 1.89 \times 10^{-4}$ (Pa^{-1})
Van Genuchten's model parameter	$n_v = 1.25$ (-)
Van Genuchten's model parameter	$m_v = 0.28$ (-)
Specific heat capacity of soil	$C_s = 880$ (J/kg/K)
Specific heat capacity of ice	$C_i = 1874$ (J/kg/K)
Specific heat capacity of water	$C_w = 4180$ (J/kg/K)
Specific heat capacity of air	$C_g = 717$ (J/kg/K)
Thermal conductivity of soil	$\lambda_s = 1.2$ (W/m/K)
Thermal conductivity of ice	$\lambda_i = 2.22$ (W/m/K)
Thermal conductivity of water	$\lambda_w = 0.58$ (W/m/K)
Thermal conductivity of air	$\lambda_g = 0.03$ (W/m/K)
Latent heat of fusion	$L_f = 3.45 \times 10^5$(J/kg)

Material properties were adopted from prior experiments [4], assuming spatial homogeneity. While this ensures compatibility with validation data, variability in properties like permeability and thermal conductivity can influence outcomes. A parametric analysis is proposed for future work.

Initially, the sample's temperature is set to 3°C. While the bottom boundary is maintained at a constant temperature, the top boundary temperature decreases to -3°C over 100 hours. Following this, the temperature rises to 3°C within 5 hours and remains constant for 15 hours. This cycle is repeated for a second round. This setup provides a comprehensive framework for evaluating soil deformation under cyclic freeze-thaw conditions.

Temperature variations

The results of temperature variation at different heights are presented in Fig. 2. The graph illustrates the variation of temperature at different heights (1 cm, 2 cm, 7 cm, and 8 cm) over time during the cyclic freeze-thaw simulation. The experimental data closely align with the numerical simulation results, confirming the model's accuracy. As shown in Fig. 2, during the first cycle, the temperature at all heights drops as the top temperature is reduced to -3°C over 100 hours. A clear thermal gradient develops, with the upper heights (e.g., 7 cm and 8 cm) cooling faster than the lower heights (e.g., 1 cm and 2 cm). When the temperature rises back to 3°C over 5 hours and stabilizes for 15 hours, the sample warms up gradually, again showing a delay in response at lower heights due to thermal diffusion and advection.

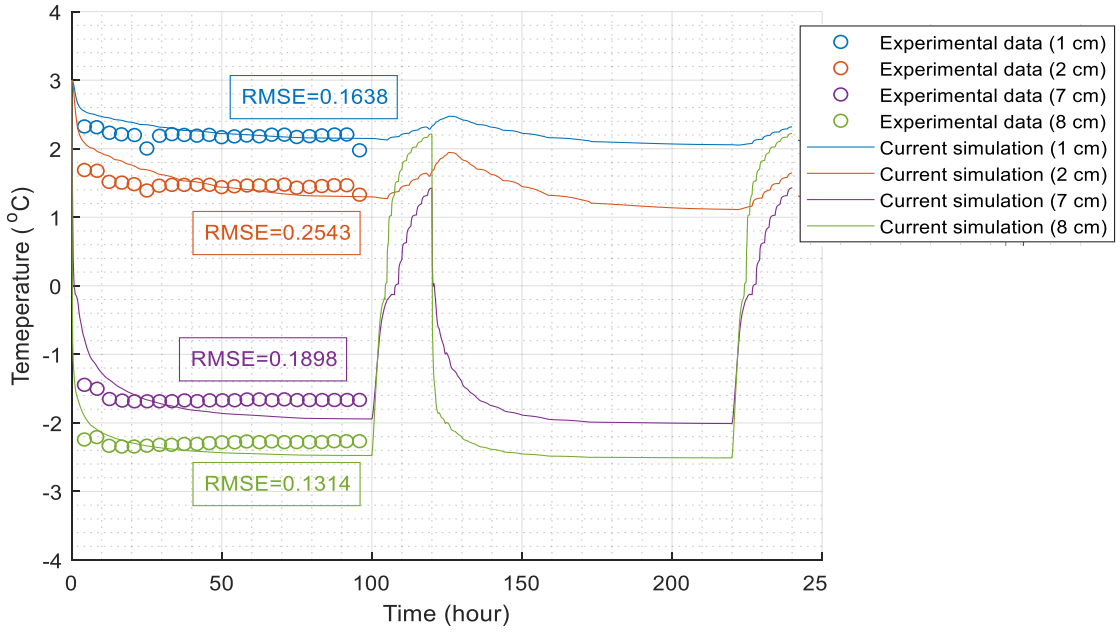

Figure 2: Temperature versus time at different heights

In the second cycle, the temperature profiles at all heights exhibit similar trends, but the changes are more uniform compared to the first cycle. This is likely due to the redistribution of

thermal energy within the sample after the first cycle, reducing the initial thermal gradients. The temperature rise and fall during the second cycle also appear slightly faster, especially near the upper heights, indicating improved thermal equilibrium. Although the trend is the same, the minimum temperature of second cycle is slightly less than the first cycle. Overall, the comparison highlights the cumulative effect of cyclic freeze-thaw processes, where subsequent cycles tend to reduce temperature gradients within the sample.

Result of displacement of sample

Figures 3 and 4 illustrate the displacement behavior of the sample during freeze-thaw cycles, with Figure 3 showing the overall displacement evolution over time and Figure 4 providing a direct comparison between the first and second cycles. During each cycle, freezing causes upward displacement due to ice formation and frost heave, while thawing leads to settlement as ice melts and pore water redistributes. The numerical simulation aligns well with experimental data during the freezing phase, capturing the gradual displacement increase.

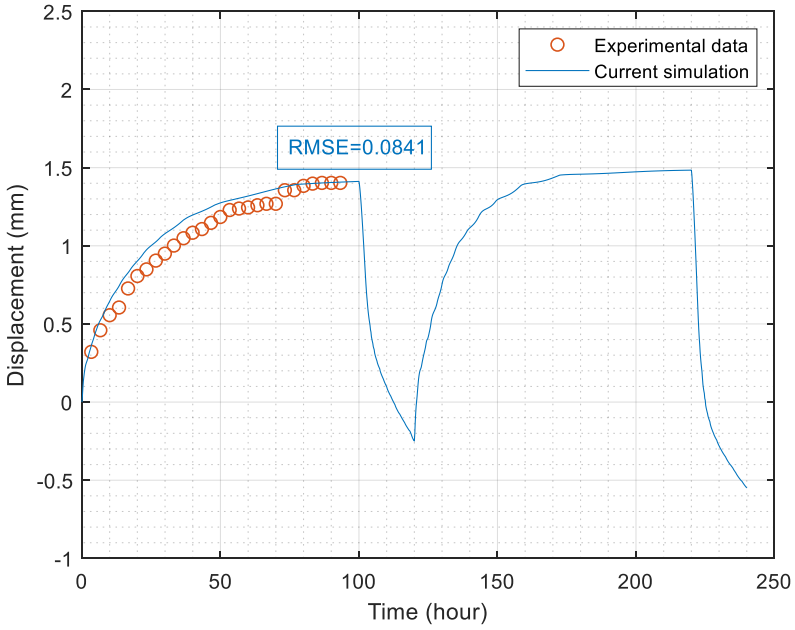

Figure 3: Numerical simulation of displacement of sample during cyclic freeze-thaw processes

In both cycles, the peak upward displacement occurs near the end of the freezing phase, reaching approximately 1.5 mm in the first cycle. Figure 4 reveals that the second cycle exhibits a slightly higher peak displacement during freezing, likely due to pore water and ice pressure redistribution and plastic deformation of the soil. Additionally, the thawing phase in the second cycle shows a faster contraction, which could be attributed to progressive soil settlement or residual deformation from the previous cycle.

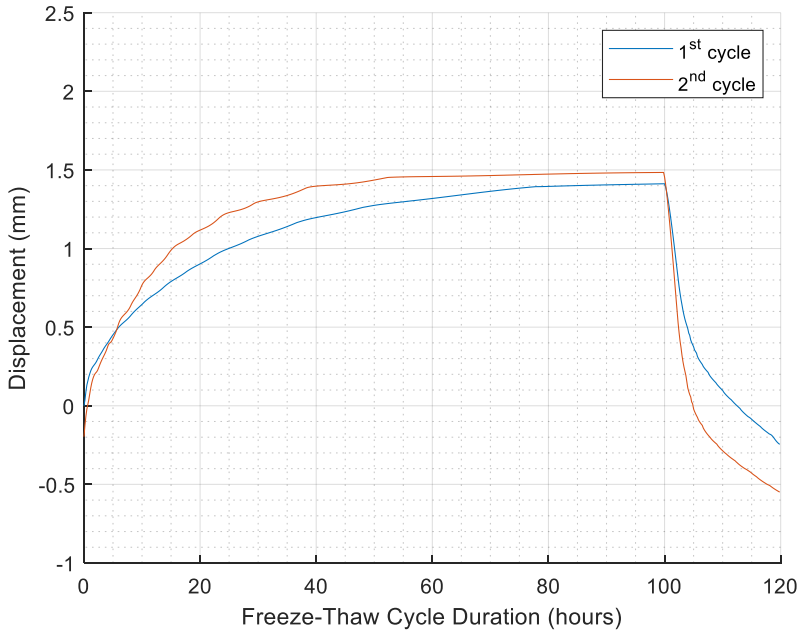

Figure 4: Comparison the displacement of the sample between the first and second cycles

Conclusions

This study investigated the THM behavior of unsaturated frozen soil subjected to cyclic freeze-thaw actions using a two-dimensional numerical model based on derived governing equations.

- The numerical model accurately simulated temperature and deformation in unsaturated frozen soil under cyclic freeze-thaw conditions, showing strong agreement with experimental data.
- Frost heave and settlement during freezing and thawing cycles, with varying displacement magnitudes, were observed. The differences between cycles were attributed to residual plastic deformation and changes in the pore structure.
- In order to study effects, it is recommended to conduct a three-dimensional model and compare the results with current simulation.
- The study highlights the importance of incorporating cumulative effects into models for better prediction accuracy, offering valuable insights for geotechnical applications in cold regions.

References

[1] Z. Li, J. Chen, A. Tang, M. Sugimoto, A novel model of heat-water-air-stress coupling in unsaturated frozen soil, Int. J. Heat Mass Transf. 175 (2021) 121375.

[2] S. Nishimura, A. Gens, S. Olivella, R.J. Jardine, Thm-coupled finite element analysis of frozen soil: Formulation and application, Geotechnique 59 (2009) 159–171. https://doi.org/10.1680/geot.2009.59.3.159.

[3] Y.W. Bekele, H. Kyokawa, A.M. Kvarving, T. Kvamsdal, S. Nordal, Isogeometric analysis of THM coupled processes in ground freezing, Comput. Geotech. 88 (2017) 129–145.

[4] R. Bai, Y. Lai, W. Pei, M. Zhang, Investigation on frost heave of saturated–unsaturated soils, Acta Geotech. 15 (2020) 3295–3306.

[5] X. Huang, D.L. Rudolph, Coupled model for water, vapour, heat, stress and strain fields in variably saturated freezing soils, Adv. Water Resour. 154 (2021) 103945.

[6] Y. Wu, T. Ishikawa, Thermal-Hydro-Mechanical coupled analysis of unsaturated frost susceptible soils, Res. Cold Arid Reg. 14 (2022) 223–234.

[7] B. Li, E. Norouzi, H.-H. Zhu, B. Wu, A thermo-poromechanical model for simulating freeze–thaw actions in unsaturated soils, Adv. Water Resour. 184 (2024) 104624.

[8] E. Norouzi, B. Li, Finite element modeling of thermal-hydro-mechanical coupled processes in unsaturated freezing soils considering air-water capillary pressure and cryosuction, Int. J. Numer. Anal. Methods Geomech. 48 (2024) 2944–2970.

[9] X. Yin, Y. Lai, E. Liu, Microstructure-based effective stress for unsaturated frozen soils, Int. J. Numer. Anal. Methods Geomech. 47 (2023) 261–274.

[10] D. Gawin, F. Pesavento, M. Koniorczyk, B.A. Schrefler, Poro-mechanical model of strain hysteresis due to cyclic water freezing in partially saturated porous media, Int. J. Solids Struct. 206 (2020) 322–339.

[11] M.T. Van Genuchten, A closed-form equation for predicting the hydraulic conductivity of unsaturated soils, Soil Sci. Soc. Am. J. 44 (1980) 892–898.

[12] E. Norouzi, B. Li, L.L. Wang, J. Raymond, A. Gaur, J. Zou, Numerical evaluation of ground source heat pumps in a thawing permafrost region, J. Build. Eng. 98 (2024) 111035. https://doi.org/https://doi.org/10.1016/j.jobe.2024.111035.

[13] E.A. de Souza Neto, R.A. Feijóo, On the equivalence between spatial and material volume averaging of stress in large strain multi-scale solid constitutive models, Mech. Mater. 40 (2008) 803–811. https://doi.org/https://doi.org/10.1016/j.mechmat.2008.04.006.